Antibiofilm effect enhanced by modification of 1,2,3-triazole and palladium nanoparticles on polysulfone membranes

Thesis by

Hong Cheng

In Partial Fulfillment of the Requirements

For the Degree of

Master of Science

August 2015 King Abdullah University of Science and Technology

Thuwal, Kingdom of Saudi Arabia

EXAMINATION COMMITTEE APPROVALS FORM

Committee Chairperson: Dr. Peiying Hong

Committee Member: Dr. Suzana Nunes

Committee Member: Dr. Peng Wang

ABSTRACT

Antibiofilm effect enhanced by modification of 1,2,3-triazole and palladium nanoparticles on polysulfone membranes

Thesis by

Hong Cheng

Biofouling impedes the performance of membrane bioreactors. In this study, we investigated the antifouling effects of polysulfone membranes that were modified by 1,2,3-triazole and palladium nanoparticles. The membranes to be tested were embedded within a drip flow biofilm reactor, and *Pseudomonas aeruginosa* PAO1 was inoculated and allowed to establish biofilm on the tested membranes. It was found that 1,2,3-triazole and palladium nanoparticles can inhibit the bacterial growth in aerobic and anaerobic conditions. The decrease in bacterial growth was observed along with a decrease in the amount of total polysaccharide and Pel polysaccharide within the biofilm matrix but not the protein content.

Keywords: *polysulfone, 1,2,3-triazole, PdNPs, antifouling*

ACKNOWLEDGEMENTS

First of all, I sincerely and heartily thank my supervisor, Dr. Peiying Hong, whose suggestions and encouragements have given me much insight into this research. It has been a great privilege and joy to study under her guidance and supervision. The same appreciation is given to my committee members Dr. Suzana Nunes and Dr. Peng Wang.

I would like to take this opportunity to express my gratitude to all the people who have helped me in this work. Especially Dr. Yanghui Xiong, Yihui Xie, Francisco Villalobos, Moustapha Harb, Zhixiong Liu, and my friendly group members. Without their kind help, I would not be able to complete this thesis.

I am also extremely grateful to my family and all my friends who have kindly provided me with assistance and companionship. I bear in mind their endless encouragement showered onto me.

TABLE OF CONTENTS

Article I. Table of Contents

LIST OF ABBREVIATIONS

MBR	Membrane bioreactors
TCE	Trichloroethene
PSU	Polysulfone
PPCPs	Pharmaceuticals and personal care products
PAHs	Polycyclic aromatic hydrocarbons
VOCs	Volatile organic compounds
COCs	Chlorinated organic contaminants
CT	Carbon tetrachloride
TCE	Trichloroethene
PCE	Perchloroethene
PCBs	Polychlorinated biphenyls
$Pd(OAc)_2$	Palladium(II) acetate
DMAc	N,N-Dimethylacetamide
$NaBH_4$	Sodium tetrahydroborate
SEM	Scanning electron microscopy
AFM	Atomic force microscopy
DFR	Drip-flow biofilm reactor
SMP	Soluble microbial products
PN	Extracellular proteins
PS	Polysaccharides
BSA	Bovine Serum Albumin
AeMBR	Aerobic membrane bioreactor
TMP	Transmembrane pressure

COD	Chemical oxygen demand
EPS	Extracellular polysaccharides substances
ATP	Adenosine triphosphate

LIST OF FIGURES

LIST OF TABLES

1.Introduction

Membrane bioreactors (MBR) are increasingly used as a preferred biotechnology in industrial wastewater treatment because the coupling of a membrane separation process would achieve an improved effluent quality. Membranes can also be used to retain biogenic metals within the bioreactors. The biogenic metals can in turn achieve a catalytic breakdown of contaminants that are not easily biodegradable. For example, Forrez and coworkers have demonstrated the reductive removal of pharmaceuticals, biocides and iodinated contrast media by palladium (Pd) (Forrez et al. 2011). Similarly, Hennebel and co-workers used Pd in a continuous plate membrane reactor to achieve a complete, efficient and rapid removal of trichloroethene (TCE) (Hennebel et al. 2009). In both instances, Pd was either physically retained in the MBR through the use of hollow-fiber nanofiltration membranes or recirculated throughout the reactor system in the form of suspension. This can result in the agglomeration of Pd nanoparticles which will cause a subsequent decrease in the catalytic effect. To overcome this limitation, Pd nanoparticles can be embedded onto membrane surfaces instead so as to achieve an even distribution of this catalyst throughout the reactive surface area. For example, Villalobos et al. have demonstrated that polymeric membranes can be loaded with metal ions or nanoparticles in a well-dispersed and uniform manner (Villalobos et al. 2013; Villalobos et al. 2015). However, this proposed strategy would mean that the Pd membrane may become susceptible to biofouling because Pd nanoparticles

have relatively weaker antibacterial effects compared to other heavy metals such as silver or copper nanoparticles (Kim et al. 2007; Ruparelia et al. 2008; Adams et al. 2014). Biofouling is particularly detrimental to the performance of membrane bioreactors as they can result in decreased permeate production, increased trans-membrane pressure and a shorter lifetime of membrane module (Flemming 1997).

In this study, we propose the embedment of Pd on the polysulfone (PSU) membrane with 1,2,3-triazole functional groups. Triazole was previously demonstrated to have antibacterial effect (Holla et al. 2005; Aufort et al. 2008; Wang et al. 2010). In addition, triazole exhibits hydrophilic functionalities that are anticipated to make the Pd-embedded PSU membranes less susceptible to proteins, fatty acids and organic fouling (Rana and Matsuura 2010). Given the antibacterial effects of Pd nanoparticles and triazole and the hydrophilic nature of triazole, we propose the Pd nanoparticles and triazole functional groups could work in synergy to improve the antifouling effects. This study aims to demonstrate that a Pd nanoparticles embedded triazole PSU membrane would show high antifouling properties.

2. Literature Review

2.1 Chlorinated organics-contaminated wastewater and conventional treatment technologies

Various types of chemical and pharmaceutical industries produce wastewater that contains compounds detrimental to humans and the environment. These waste products include aromatic pharmaceuticals and personal care products (PPCPs), polycyclic aromatic hydrocarbons (PAHs) and volatile organic compounds (VOCs). Among these contaminants, chlorinated organic contaminants (COCs) including carbon tetrachloride (CT), trichloroethene (TCE), perchloroethene (PCE), polychlorinated biphenyls (PCBs) constitute a large portion of the waste products generated by chemical industries (Zhang et al. 1998).

Local regulations in many countries require the wastewater from industries to be first treated until the quality is within the permissible levels prior to discharge to sewage pipelines. To achieve the required effluent quality, traditional treatment technologies applied to COCs include physical, chemical and biological methods (Chaplin et al. 2012). However, these technologies have their own drawbacks. To illustrate, activated carbon absorption is a widely used physical technology that can extract contaminants from wastewater to a solid phase. However, this treatment method is simply a transfer of an aqueous contamination problem to a solid waste issue. Furthermore, it needs subsequent processes to recover the activated carbons

for reuse (Rafatullah et al. 2010). Alternatively, oxidation can also be used to treat organic contaminants. However, oxidants have poor selectivity for COCs and this limitation will increase the cost of treatment (Chaplin et al. 2012).To further compound the problem, oxidation of organic rich wastewater can produce many kinds of byproducts that can be toxic and carcinogenic (Richardson et al. 2007).

As for biological technology, the efficiency of biodegrading COCs by microorganisms takes a long time and may not be cost-effective. To circumvent this limitation, membrane separation process can be integrated to a bioreactor to achieve physical separation of organic contaminants. The integrated membranes can also serve to retain the biomass within the bioreactor, hence achieving higher mixed liquor suspended solids content to biodegrade the high organic load. Membranes can also be coated or embedded with catalyst (e.g. Pd) to accelerate degradation rates of COCs (Wang et al. 2008).

2.2. Palladium catalysis effects

Pd is a noble metal, conventionally used for dechlorination. Pd-based catalysis coupled with H_2 gas is a potential strategy to treat COCs (Tab. 1).

Table 1. Palladium-based catalysis used to treat chlorinated organic contaminants in previous studies.

Type of COCs treated by Pd catalysis	End products	references
1,1,1- $C_2H_2Cl_3$	C_2H_6 /C_2H_4	(Lien and Zhang 2005)
1,1,1,2-$C_2H_2Cl_4$	C_2H_6 /C_2H_4	(Lien and Zhang 2005)
1,1,2,2- $C_2H_2Cl_4$	C_2H_6 /C_2H_4	(Lien and Zhang 2005)
3,3,4,4-tetrachlorobiphenyl	Biphenyl	(Venkatachalam et al. 2008)
C_2Cl_6	C_2H_6 /C_2H_4	(Lien and Zhang 2005)
C_2HCl_5	C_2H_6 /C_2H_4	(Lien and Zhang 2005)
para-nitrochlorobenzene	Aniline	(Dong et al. 2011)
PCE	C_2H_6	(Kustov et al. 2011)
TCE	C_2H_6 /C_2H_4	(Nutt et al. 2006)
Trichloroacetic acid	Acetic acid	(Wang et al. 2008)

Pd-based catalysis decomposes COCs through hydrodehalogenation reaction. The proposed reaction pathways are shown in Fig. 1. Pd-based catalysis is highly effective in dehalogenating a variety of contaminants, especially COCs, without producing toxic byproducts. Pd-based catalysis also provides rapid reaction rates (Lowry and Reinhard 2000). In particular, Pd nanoparticles, with a size ranging from 1 to 100 nm have exhibited unique chemical and physical properties. Compared to the Pd ions and metal, the Pd nanoparticle shows excellent catalytic

effeciency. For instance, Lien and co-workers used nanoscale Pd particles to treat chlorinated ethanes, and achieved hydrodechlorination of several chlorinated ethanes such as hexachloroethane, pentachloroethane, 1,1,2,2-tetrachloroethane in less than one hour (Lien and Zhang 2005). Wong et al. also successfully designed a Pd/Au bimetallics which was able to effectively remove TCE in the aqueous phase (Wong et al. 2005).

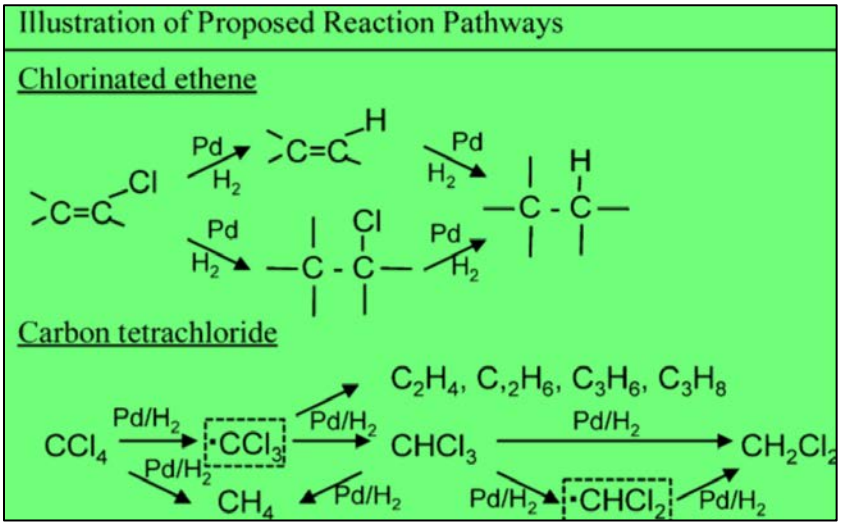

Figure 1. The proposed reaction pathways of Palladium-based catalysis (Adapted from (Chaplin et al. 2012)).

2.3. Limitations of palladium-based catalysis and potential solutions

Even though Pd nanoparticles are one of potential catalysts to treat COCs, there are still some technical bottlenecks to be resolved. These bottlenecks include aggregation of Pd nanoparticles that will result in a decrease of catalysis efficiency. Additionally, recycling Pd nanoparticles from the reaction agent or water is very difficult. Considering Pd is noble metal, recovery of this particle for regeneration and reuse is particularly essential for cost-effectiveness. However, for the conventional strategy of using Pd nanoparticles, it is hard to separate and extract the added nanoparticles because of their small size. Lastly, discharging of Pd nanoparticles in the treated effluent streams may result in environment concerns. Speranza and co-workers demonstrated that Pd showed higher toxicity than Pd ions to plants by changing the morphology of pollens (Wang et al. 2008; Speranza et al. 2010; Zhao et al. 2011). Hence, to overcome these limitations and bottlenecks, chelating Pd nanoparticles onto membranes is an ideal solution (Fig. 2).

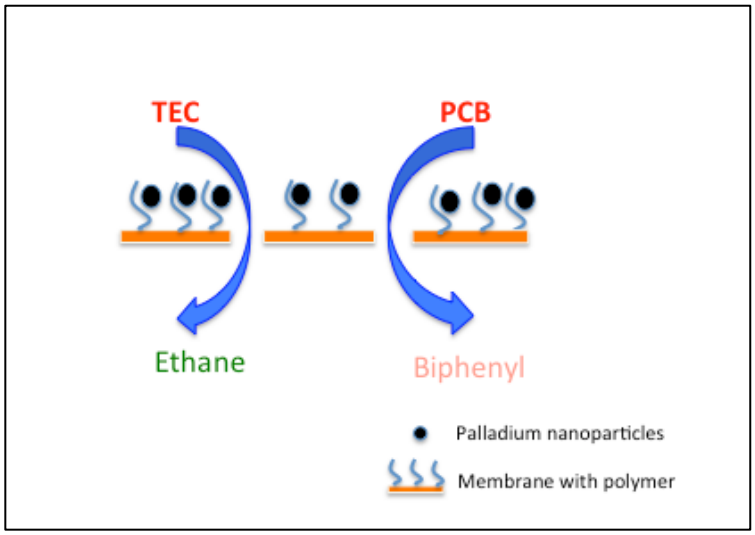

Figure 2. Schematic of palladium nanoparticles embedded membrane treating chlorinated organic contaminants.

There are several advantages of embedding nanoparticles onto membranes, namely: i) easy control of the nanoparticles concentration; ii) uniform distribution of the nanoparticles by preventing undesirable aggregation, and iii) minimize dispersal of Pd into environment. Due to these merits, immobilization of nanoparticles onto membranes has drawn extensive interests. For example, Villalobos et al. have exhibited a polymeric membrane that can be loaded with metal ions or nanoparticles in a well-dispersed and uniform manner (Villalobos et al. 2013; Villalobos et al. 2015). Hennebel and the co-workers have developed a membrane reactor containing bio-Pd nanoparticles for removal of TCE, and up to 2500 mg TCE can be removed per day per gram of Pd nanoparticles and with H_2 acting as the hydrogen donor (Hennebel et al. 2009). Wang et. al successfully immobilized Pd

nanoparticles onto the Poly(vinylidene fluoride)(PVDF) microfiltration membrane and they showed that this new membrane can remove trichloroacetic acid effectively (Wang et al. 2008).

2.4 Biofouling on palladium-based membrane systems

Based on earlier studies as summarized in the earlier section, Pd nanoparticle-embedded membranes has shown many advantages for application to treat COCs contaminants. Nonetheless, the long-term operational durability of such membranes in a bioreactor should be considered. Membrane systems are generally prone to form biofilms on the membrane surfaces (i.e., membrane fouling) because water, especially wastewater, contains many kinds of microorganisms, organic and inorganic matters. The fouling not only decreases permeate flux of water production and increase trans-membrane pressure, but also shorten the lifetime of membrane module (Flemming 1997). In addition, fouling will prevent contact between Pd and contaminants, resulting in deactivation of Pd nanoparticle catalysts.

Numerous factors can cause fouling. Particulates can physically attach onto the surface of membranes to form a cake layer. Inorganic or organic matter including humic acids, fulvic acids and some protein can bind to membrane surfaces or membrane pores. Bacteria, fungus, algae can also attach onto the membranes and result in membrane biofouling (Guo et al. 2012). Among all kinds of fouling, biofouling is thought to be the worst problem since it is not only difficult to remove but also contributes to more than 45% of the whole fouling event in a membrane bioreactor (Komlenic 2010).

Biofouling development is generally comprised of five steps: i) initial attachment of cell to the surface; ii) irreversible attachment of cells; iii)

development of biofilm structure; iv) maturation of biofilm architecture; v) single cells dispersal from biofilm (Davies et al. 1998; Stoodley et al. 2002).

Given the serious problems associated with fouling, decreasing or eliminating the formation of biofilm has attracted extensive research interests. Many strategies were offered to control fouling, such as pretreatment of water (e.g. coagulation, adsorption, pre-oxidation, disinfection), operating membrane systems with optimal parameters, chemical cleaning and so on (Gao et al. 2011). Recently, modification of membrane characteristics was proposed and showed much potential. Nanoparticles coating and surface functionalization are two common strategies used in membrane modification. Nanoparticles are well known for their antibacterial activity. Many nanoparticles such as silver nanoparticles, TiO_2, SiO_2, CuO, ZnO, MgO, carbon nanotubes have been illustrated to possess antibacterial activity (Banerjee et al. 2011). However, only few studies focused on the antimicrobial capacity of Pd nanoparticles (Adams et al. 2014).

Apart from nanoparticles coating, changing membrane surface with functional groups is another ideal strategy. In particular, changing the membrane surface from hydrophobic to hydrophilic can effectively prevent biofilm forming. This is because EPS, which play a significant role in anchoring bacteria cells to membrane surface by bridging across the repulsion barrier, are comprised of hydrophobic organic compounds. Furthermore, as cell surface of bacteria was demonstrated to be relatively hydrophobic, this means that bacteria are able to attach onto hydrophobic membranes more easily (Marshall 1985). As such, modifying membrane surfaces to

become hydrophilic can lower biofouling potential (Park et al. 2005). One potential functional group to modify onto membrane surfaces to increase hydrophilicity would be the triazole. Triazole ligand is known for its hydrophilic nature and it can attach onto PSU backbone to form a tight hydrogen layer on surface. The triazole-modified PSU membrane shows hydrophilic instead of hydrophobic nature, which is in turn anticipated to be less prone to biofouling events (Xie et al. 2015)(Tab.2).

Table 2. Contact angle of membranes (Adapted from Xie et al. 2015)

Membranes	Contact angle (◦)
PSU-TriN-0%	80.7±2.5
PSU-TriN-23%	77.0±0.2
PSU-TriN-49%	74.5±1.3
PSU-TriN-94%	70.0±2.0

This is because hydrophilic membrane surfaces can prevent organics and bacteria, both of which are hydrophobic, from attaching onto membranes (Fig. 3).

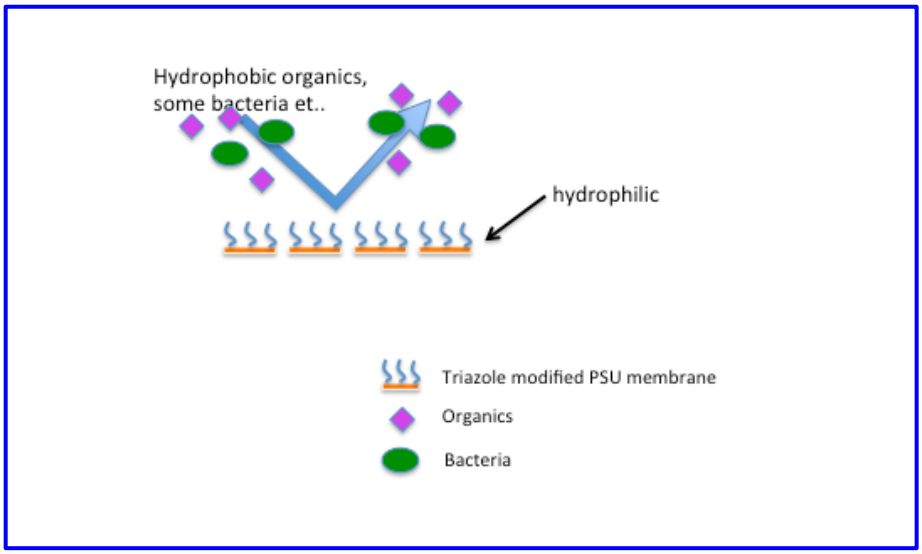

Figure 3. Triazole-modified membrane can reject the hydrophobic matters.

3. Materials and Methods

3.1 Membranes

Six types of PSU membranes were tested for the extent of biofilm formation. This includes four different concentrations of triazole (i.e., 0%, 23%, 49% and 94%) functionalized onto PSU membranes. These membranes were named in this thesis as PSU-TriN-0%, PSU-TriN-23%, PSU-TriN-49%, PSU-TriN-94%, based on the triazole concentrations functionalized onto it. Also two PSU-TrN-94% membranes containing palladium ions (PSU-TriN-Ions) and palladium nanoparticles (PSU-TriN-NPs), respectively, were evaluated in this study.

PSU-TriN with different concentrations of triazole was synthesized following a method published by Xie et al. Briefly, polysulfone was chloromethylated in the presence of phenyl rings and 1,4-disubstituted 1,2,3-triazole rings were incorporated by copper(I)-catalyzed azide-alkyne cycloaddition (Xie et al. 2015). PSU-TriN-0%, PSU-TriN-23%, PSU-TriN-49%, and PSU-TriN-94% membranes were made by non-solvent induced phase separation using water as the non-solvent, and 20 wt% polymer solutions in N,N-Dimethylacetamide (DMAc). For all of them, polyester non-woven was used as a support. The thickness of the polymer solution films casted over the non-woven was 200 μm for all the cases. All membranes were kept in deionized water before using. PSU-TriN-Ions and PSU-TriN-NPs membranes were made by complexation-induced phase separation (Villalobos et al. 2015) using Pd(II) acetate ($Pd(OAc)_2$) as the source of palladium. Briefly, (i) a 200 μm film of

polymer solution (20 wt% PSU-TrN-94% in DMAc) was casted over a nonwoven support; (ii) the resulting polymer solution film was immersed for 3 s in a 36 mM solution of $Pd(OAc)_2$ in DMAc to form the palladium rich top layer, and (iii) finally it was immersed in a subsequent water bath to form the palladium-free porous support. At this point, the PSU-TriN-Ions membrane was obtained. An additional reduction step was done to reduce the palladium ions to nanoparticles and obtain PSU-TriN-NPs. This step consisted of immersing PSU-TriN-Ions for 5 min in a 0.05M solution of sodium tetrahydroborate (NaBH4). All membranes were kept in deionized water before using.

3.2 Membrane characterization

The FEI Nova Nano scanning electron microscope (SEM)(Oregon, USA) was used to observe the surface of membranes at 5 kV. A piece of membrane sample was dried in air and then fixed onto a flat aluminum stub by tapes. Iridium was sputtered onto the membrane surface by a K575X Emitech equipment (Kent, UK) to achieve a 3 nm thickness coating.

Atomic force microscopy (AFM) was used to characterize the membrane surface topography. The membrane was dried in air and subsequently fixed onto a glass slide. AFM imaging was performed by Bruker Dimension ICON equipment (Santa Barbara, CA USA) with a soft tap mode. For each membrane, a picture with 5 μm width and 5 μm length was scanned.

3.3. Bacterial model

Pseudomonas aeruginosa PAO1 was used in this study to establish a single bacterial species biofilm matrix on membranes. It is well-documented that *P. aeruginosa* is an ideal model bacteria in biofilm research. The *P. aeruginosa* biofilm is composed of lipids, protein, extracellular DNA and exopolysaccharides. In all the constituents, the exopolysaccharides take an imperative role in biofilm architecture. There are three main exopolysaccharides (i.e. Psl, Pel and alginate) produced by *P. aeruginosa*. Among the three exopolysaccharides, Pel attributes to cell density of biofilm and accounts for about 50% of the whole polysaccharide constituent (Stoodley et al. 2002; Ghafoor et al. 2011).

3.4 Reactor setup and membrane harvesting

Drip-flow biofilm reactor (DFR) (Biosurface technologies corporation, Bozeman, Montana, USA) was used to grow biofilm. The methods and conditions were as described previously (Xu et al. 1998; Goeres et al. 2009). In brief, *P. aeruginosa* PAO1 was inoculated into 20 mL LB Broth (Lennox) (Sigma-Aldrich Co. LLC, St. Louis, MO, USA), and the growth culture was incubated in a 200 rpm shaker incubator for 24 h at 37 ^{o}C. After that, the bacterial culture was diluted with LB broth to an OD_{600} of 0.07. This OD measurement at 600 nm wavelength corresponds to an approximate cell density of 10^{8} cells/mL. The membranes were tested in

duplicates, and attached onto polycarbonate coupons. The coupons were then placed into individual channels of autoclaved DFR, and incubated for 10 h at 37 ^{o}C and in the presence of a continuous 0.8 mL/min flow of LB broth. For anaerobic condition, 1% potassium nitrate w/v was added to LB broth to ensure the growth of *P. aeruginosa* PAO1 in the presence of nitrate as an alternative electron acceptor (Toyofuku et al. 2012). The membranes were harvested after 48 h of cultivation in aerobic condition, and after 72 h of cultivation due to a slower growth rate under anaerobic condition.

Four batches including two aerobic and two anaerobic conditions were conducted. The biofilm grew homogeneously throughout the entire membrane surface in aerobic condition but not in anaerobic condition. As such, actual area of biofilm was calculated by Image J software before harvesting in anaerobic condition.

The membranes were harvested and handled in slightly different manner for the individual duplicates. Briefly, one membrane was washed by 40 mL of 1X phosphate buffer saline (PBS) to remove the loosely-bound biofilm and the other membrane was placed into 40 mL PBS without any prior washing step (i.e., both loosely- and strongly-bound biofilm were collected). The tubes containing loosely-bound biofilm and total biofilm were individually ultrasonicated for 3 min by a Q500 sonicator (Qsonica) at 25% amplitude to disperse biofilm into the liquid suspension. The membranes were then removed from the liquid suspension and the suspension was analyzed for their contents based on protocols described in section 3.6 through 3.8.

3.5 Image acquisition

The membranes with the strongly-bound biofilm were stained by the LIVE/DEAD ® BacLight TM Bacterial Viability and Counting Kit (L34856) (Thermo Fisher Scientific Inc., Waltham, MA, USA) for 20 min. Zeiss LSM 710 (Carl Zeiss Microscopy GmbH, Jena, Germany) with 20X magnification objective was used. Image scanning was carried out with the 488 nm and 561 nm laser line from an Ar/Kr laser. In all the experiments, 7 different images for each membrane were obtained and the pictures were analyzed by Image J software. In short, each picture was split into two pictures according the different channels (i.e. red and green). Then the dead cells and live cells were respectively counted by the pixels of picture and live/dead ratio was calculated.

3.6 Live cell counting

1 mL of the liquid suspension was aliquot and diluted by 5000 to 7000-fold in 1X PBS for flow cytometry on Accuri C6 (BD Bioscience, NJ, USA). LIVE/DEAD ® BacLight TM Bacterial Viability and Counting Kit (L13152) (Thermo Fisher Scientific Inc., America) was used to stain the bacteria based on manufacturer's protocol. Briefly, 300 µL of the 2X propidium iodide: Syto9 dye with respective concentrations of 30 µM and 6µM was added to 300 µL of diluted liquid suspension and incubated in room temperature and in the dark for 15 min before flow

cytometry. 50 µL stained samples were injected with 35 µL/min rate to enumerate cells with intact cell walls (i.e., live cells).

3.7 Extracellular proteins (PN) and polysaccharides (PS)

The supernatant was first filtered through 0.22 µm syringe filter (VWR Int., Radnor, PA, USA) prior to determination of its PN and PS. PN was quantified by Total Protein Kit, Micro Lowry, Peterson's Modification (TP0300, Sigma-Aldrich, America) based on the Lowry method (Randall and Lewis 1951), with 0 µg/mL, 10 µg/mL, 20 µg/mL, 40 µg/mL and 80 µg/mL of Bovine Serum Albumin (BSA) as standard and measured in triplicates. PS was determined by the phenol-sulfuric acid method and 0 µg/mL, 5 µg/mL, 10 µg/mL, 20 µg/mL, 40 µg/mL and 80 µg/mL glucose were used as standards (DuBois et al. 1956).

3.8 Pel polysaccharides test

Congo red binding assay was performed to assess the Pel polysaccharides concentration within the biofilm matrix of each membrane (Ghafoor et al. 2011). Prior to analysis, the liquid suspension was briefly vortex to ensure homogeneity in the contents. 10 mL of the homogeneous suspension was aliquot into new 50 mL tubes, centrifuged at 10000 x g for 10 min and discarded of their supernatant. The cell pellet was resuspended in 10 mL of 40 mg/mL Congo red LB broth and

incubated for 90 min in a 37 ^{o}C shaker incubator. After this, the bacteria and bound Congo red were centrifuged at 10000 x g for 10 min, and the supernatant was pipetted to measure for its optical density at 490 nm. LB broth containing 5mg/mL, 10mg/mL, 20mg/mL, 40mg/mL, and 80mg/mL Congo red were also tested by optical density at 490 nm to establish a standard curve for every experiment.

4 Results

4.1 Membrane characterizations

From the SEM pictures, the PSU-TriN-0%, PSU-TriN-23%, PSU-TriN-49% and PSU-TriN-94% membranes had relatively smoother membrane surface than PSU-TriN-Ions and PSU-TriN-NPs membranes (Fig. 4). In particular, the two and three-dimensional AFM Images showed that PSU-TriN-0%, PSU-TriN-23%, PSU-TriN-49% and PSU-TriN-94% had a smoother surface topography (Fig. 5A-D) while PSU-TriN-Ions and PSU-TriN-NPs had highly uneven topography (Fig. 5C and D). This observation was also supported quantitatively by the surface roughness (Tab. 2) PSU-TriN-Ions and PSU-TriN-NPs membranes had about three-fold higher roughness arithmetic averages (R_a) than PSU-TriN-23%, PSU-TriN-49%, PSU-TriN-94% membranes and about 9-fold higher than PSU-Tri-0% membrane, Among all tested membranes, the PSU-TriN-NPs membrane showed the roughest surface topography (R_a=58.9).

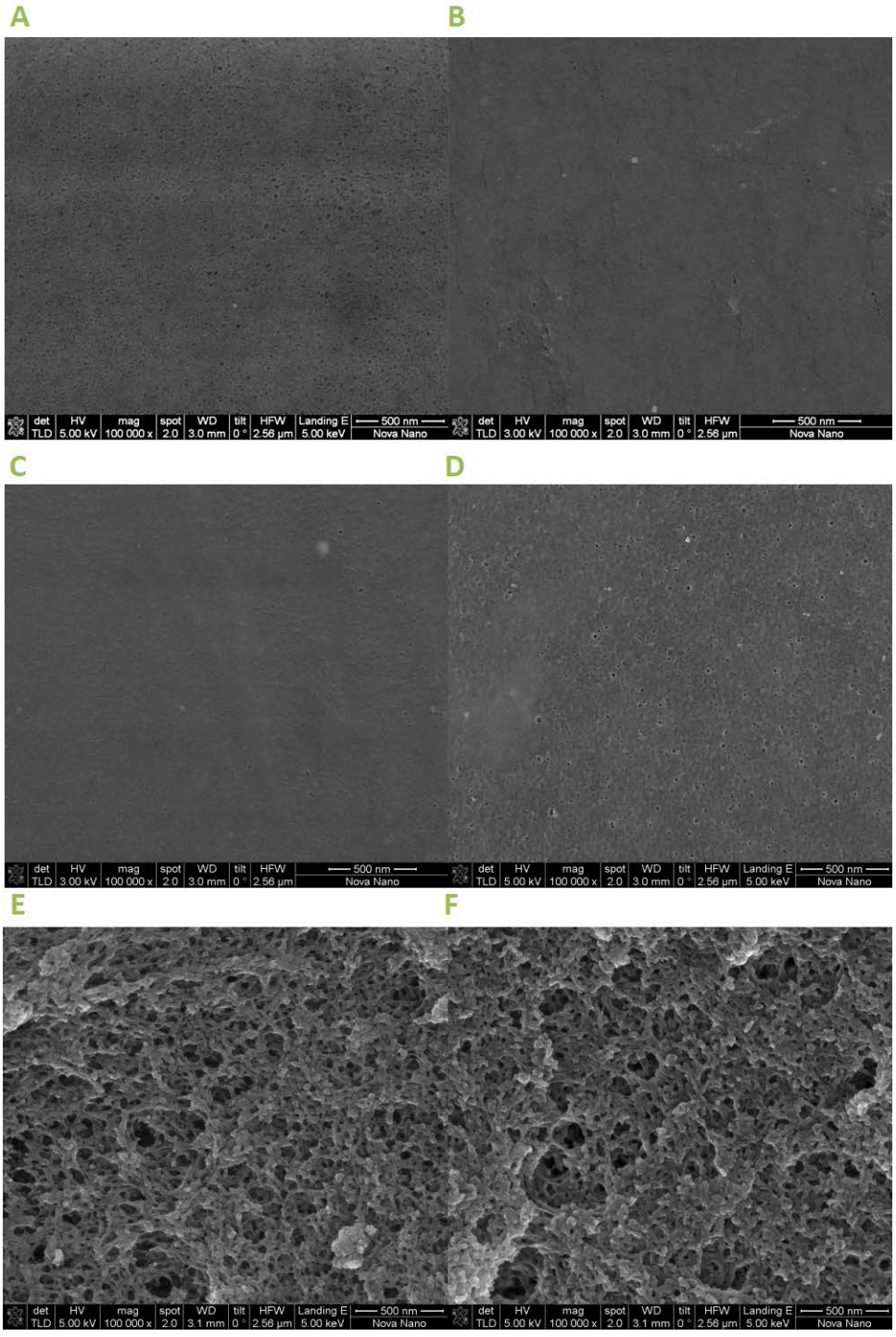

Figure 4. Scanning Electron Microscope (SEM) images of different membranes. (A)PSU-TriN-0%; (B)PSU-TriN-23%; (C)PSU-TriN-49%; (D)PSU-TriN-94%; (E)PSU-TriN-Ions;(F)PSU-TriN-NPs.

A"

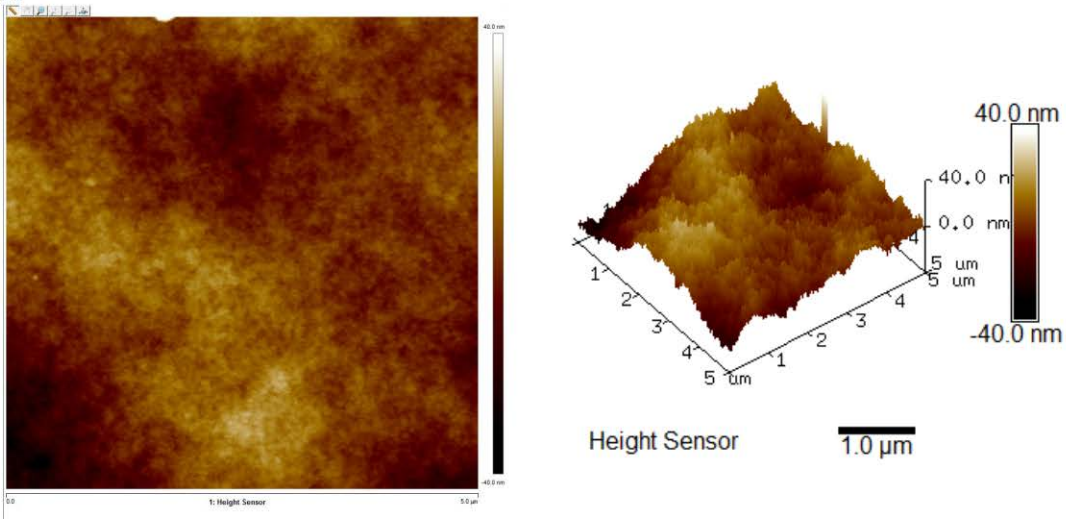
40.0 nm
40.0 nm
0.0 nm
-40.0 nm
5 um
5 um
Height Sensor
1.0 µm

B"

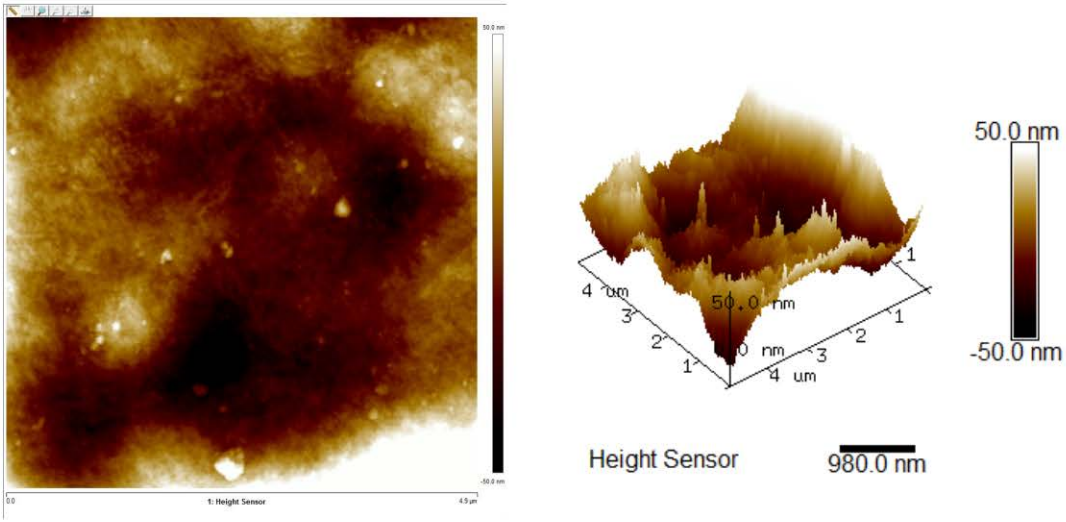
50.0 nm
-50.0 nm
Height Sensor
980.0 nm

C"

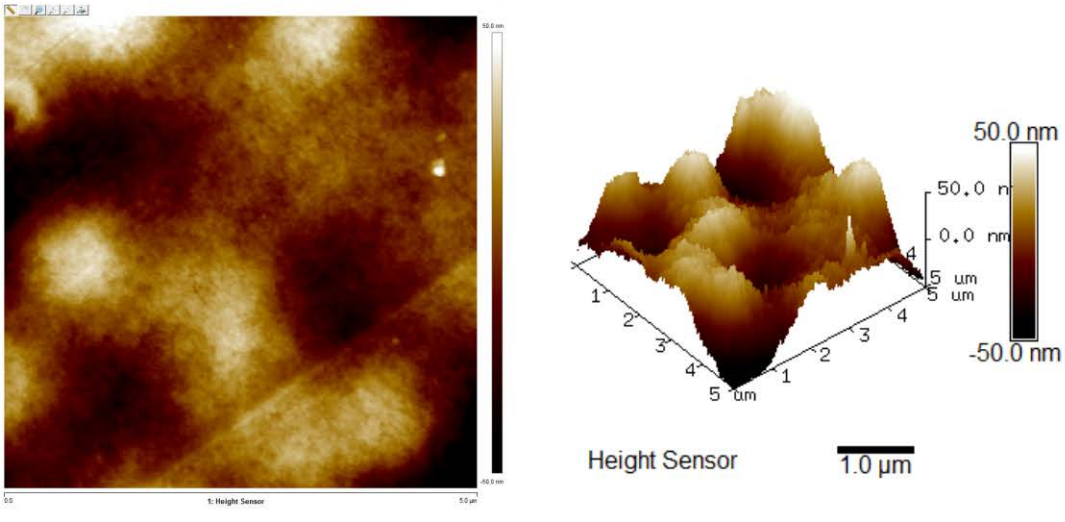
50.0 nm
50.0 nm
0.0 nm
-50.0 nm
5 um
5 um
Height Sensor
1.0 µm

D"

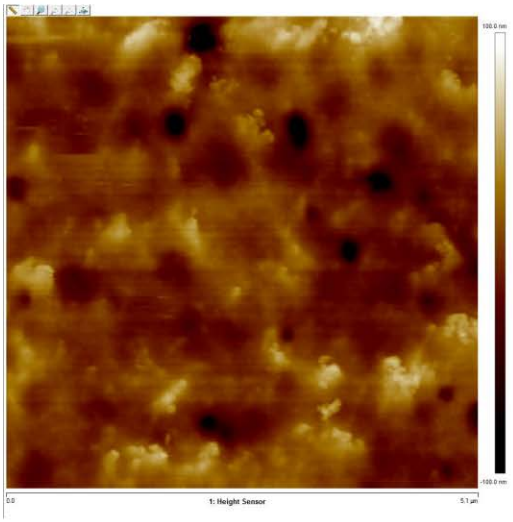
100.0 nm
100.0
0.0 nm
-100.0 nm
4.8 um
4.8 um
1.2
2.4
3.6
4.8 um
1.2
2.4
3.6
Height Sensor
1.0 µm

E"

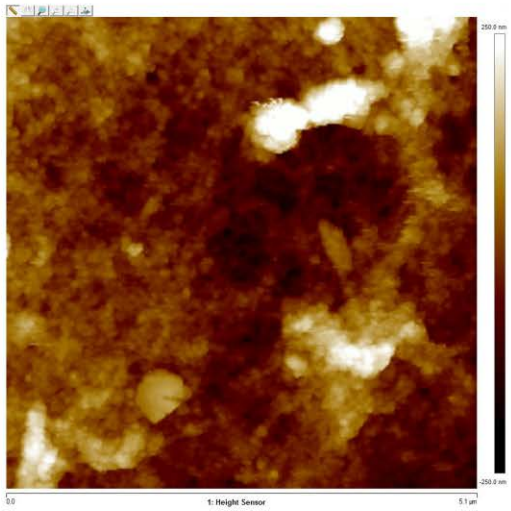
250.0 nm
250.0
0.0 nm
-250.0 nm
4.8 um
4.8 um
1.2
2.4
3.6
4.8 um
1.2
2.4
3.6
Height Sensor
1.0 µm

F"

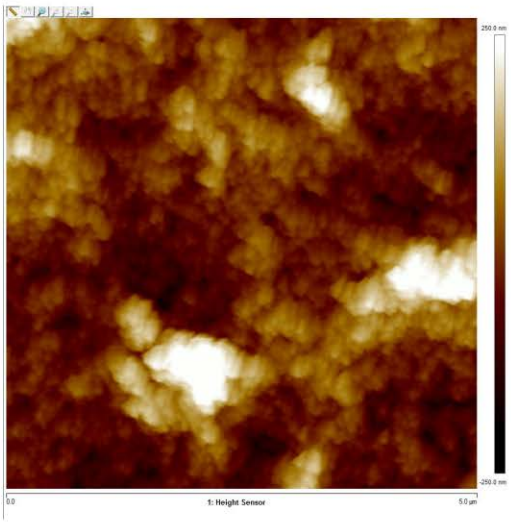
250.0 nm
250.0
0.0 nm
-250.0 nm
5 um
5 um
1
2
3
4
5 um
1
2
3
4
Height Sensor
1.0 µm

Figure 5. Atomic Force Microscopy (AFM) images of different membranes. (A)PSU-TriN-0%;(B)PSU-TriN-23%;(C)PSU-TriN-49%;(D)PSU-TriN-94%;(E)PSU-TriN-Ions;(F)PSU-TriN-

Table 3. Roughness parameters as determined by Atomic Force Microscopy.

Membrane	R_a (nm)[a]	R_q (nm)[b]	Image Z Range (nm)[c]
PSU-TriN-0%	6.35	8.26	107
PSU-TriN-23%	17.6	22.1	159
PSU-TriN-49%	14.7	18.3	114
PSU-TriN-94%	15.7	21.4	292
PSU-TriN-Ions	56.8	76.3	543
PSU-TriN-NPs	58.9	78.8	583

[a] R_a is the arithmetic average of the absolute values of the surface height deviations measured from the mean plane.

[b] R_q is the root mean square average of height deviation taken from the mean image data plane.

[c] Z range is the distance of highest peak and lowest point.

4.2 Cells quantification in biofilm matrix.

Live-dead ratio attached on membranes determined from confocal imaging. Fig. 6A and B showed that the live/dead ratio of microorganisms within the biofilm matrix of PSU-TriN-0% was higher than 1 in both aerobic and anaerobic condition (Fig. 6A and B). In contrast, the ratio of PSU-TriN-23%, PSU-TriN-49%, PSU-TriN-94% were less than 1, and were respectively significantly lower than the PSU-TriN-0% membranes (t-test, $P<0.05$). This suggested that there were less intact cells when triazole was functionalized onto the PSU membranes. In addition, PSU-TriN-NPs

showed a further reduction of live/dead ratio when compared to PSU-TriN-94% in both aerobic and anaerobic conditions (Fig. 6C and D). Further comparison with PSU-TriN-94% membrane found the Pd nanoparticles can decrease live/dead ratio significantly in aerobic (t-test, P=0.00) and anaerobic conditions (t-test, P=0.01). The PSU-TriN-Ions membrane could also further reduce the live/dead ratio when compared to PSU-TriN-94% membrane (t-test, P<0.05 in both aerobic and anaerobic conditions).

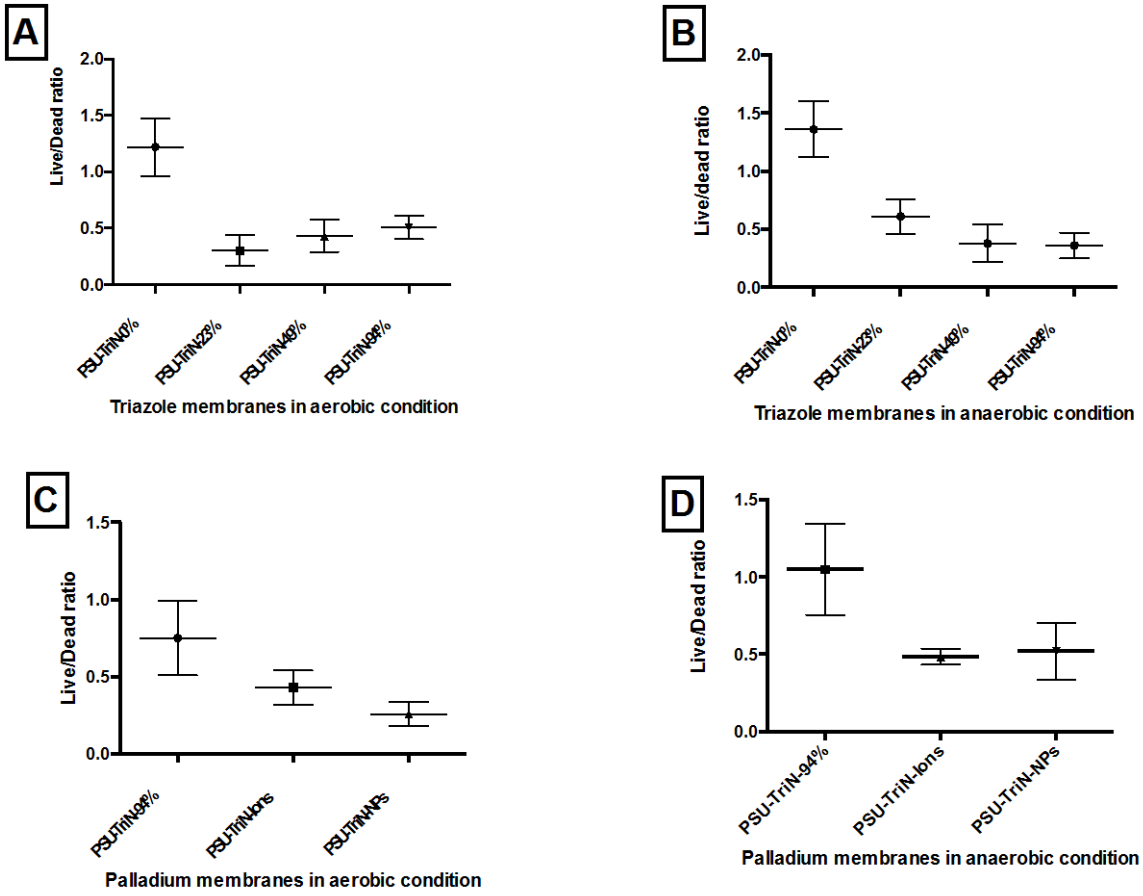

Figure 6. Live/dead ratio of bacteria attached on different membranes. (A)Different concentrations of triazole polysulfone membranes were tested in aerobic condition. (B)Four different concentrations of triazole polysulfone membrane in anaerobic condition. (C)PSU-TriN-

94%, PSU-TriN-Ions, and PSU-TriN-NPs membranes were quantified in aerobic condition. (D)PSU-TriN-94%, PSU-TriN-Ions and PSU-TriN-NPs membranes in anaerobic condition.

Live cells in biofilm matrix were also enumerated by flow cytometry. PSU-TriN-23%, PSU-TriN-49% and PSU-TriN-94% can greatly inhibit the number of live *P. aeruginosa* cells in aerobic (Fig. 7A) and anaerobic conditions (Fig. 7B). In particular, live cells on the biofilm of PSU membranes (PSU-TriN-0%) were about 5 folds higher in aerobic and approximately 8 folds higher in anaerobic conditions compared to the remaining three membranes. A higher portion of the total biofilm was loosely bound in the aerobic condition compared to anaerobic condition (Fig. 7A and B). In addition, the cells in tightly-bound biofilm on the PSU-TriN-O% membrane were higher than on the PSU-TriN-23%, PSU-TriN-49% and PSU-TriN-94% membranes (up to 2.7×10^8 cells/mL in aerobic condition and 3.95×10^8 cells/(mL*cm^2) in anaerobic condition).

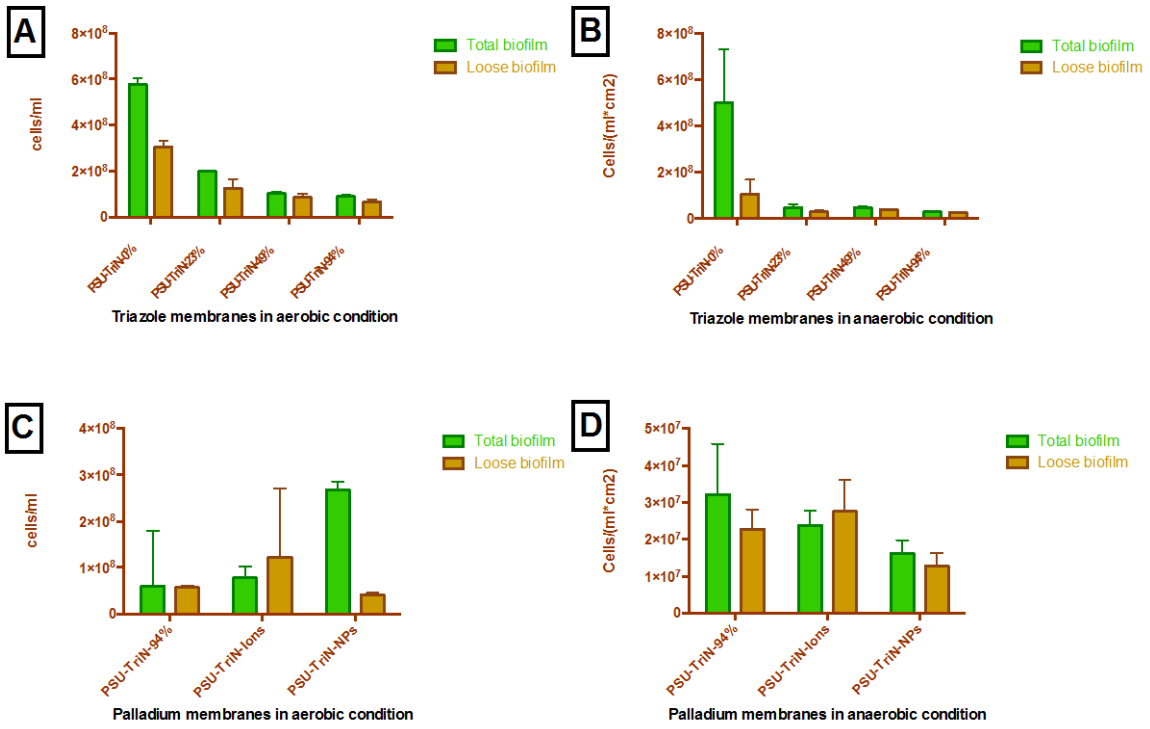

Figure 7. Live cells in the biofilms by flow cytometry. Similarly, (A)Different concentrations of traizole membranes in aerobic condition. (B)Four different triazole concentration including 0%, 23%, 49% and 94% membranes were conducted in anaerobic. (C)PSU-TriN-94%, PSU-TriN-Ions, and PSU-TriN-NPs in aerobic condition. (D)PSU-TriN-94%, PSU-TriN-Ions, and PSU-TriN-NPs in anaerobic condition**.**

A further comparison of PSU-TriN-94% membranes with PSU-TriN-NPs membranes in anaerobic condition (Fig. 7D) showed that the cells on PSU-TriN-NPs were significantly lower than on PSU-TriN-94% (t-test, P=0.02). Under aerobic condition (Fig. 7C), the cells of total biofilm on PSU-TriN-NPs membranes were higher than that detected on PSU-TriN-94% and PSU-TriN-Ions. However, the cells of loosely-bound biofilm on the PSU-TriN-NPs membrane were significantly lower to PSU-TriN-94% membranes in aerobic condition (t-test, P=0.02), suggesting that

the Pd nanoparticles were effective in affecting the loosely-bound portion of the biofilm under aerobic conditions.

As for the PSU-TriN-Ions membranes, no significant differences in the total and loosely-bound biofilm group were observed when compared with PSU-TriN-94% membranes in both aerobic and anaerobic conditions (t-test, P values were respectively 0.12, 0.30) (Fig. 7C and D).

4.3 Biofilm polysaccharides and protein quantification

Fig. 8A and B showed that for both aerobic and anaerobic conditions, the triazole membranes (i.e. PSU-TriN-23%, PSU-TriN-49%, PSU-TriN-94%) could inhibit the polysaccharides production. Statistical analysis revealed significant differences between PSU-TriN-0% and PSU-TriN-23%, PSU-TriN-49%, PSU-TriN-94% membranes (t-test, all $P<0.03$). A significant difference could also be obtained between PSU-TriN-94% and PSU-TriN-NPs membranes (Fig. 8C and D, t-test, P=0.01, 0.02 respectively). However, there was no significant difference between PSU-TriN-94% and PSU-TriN-Ions membranes (t-test, P=0.12, 0.13 respectively in aerobic and anaerobic conditions). It is likely PSU-TriN-Ions membrane could not effectively inhibit the production of

polysaccharides.

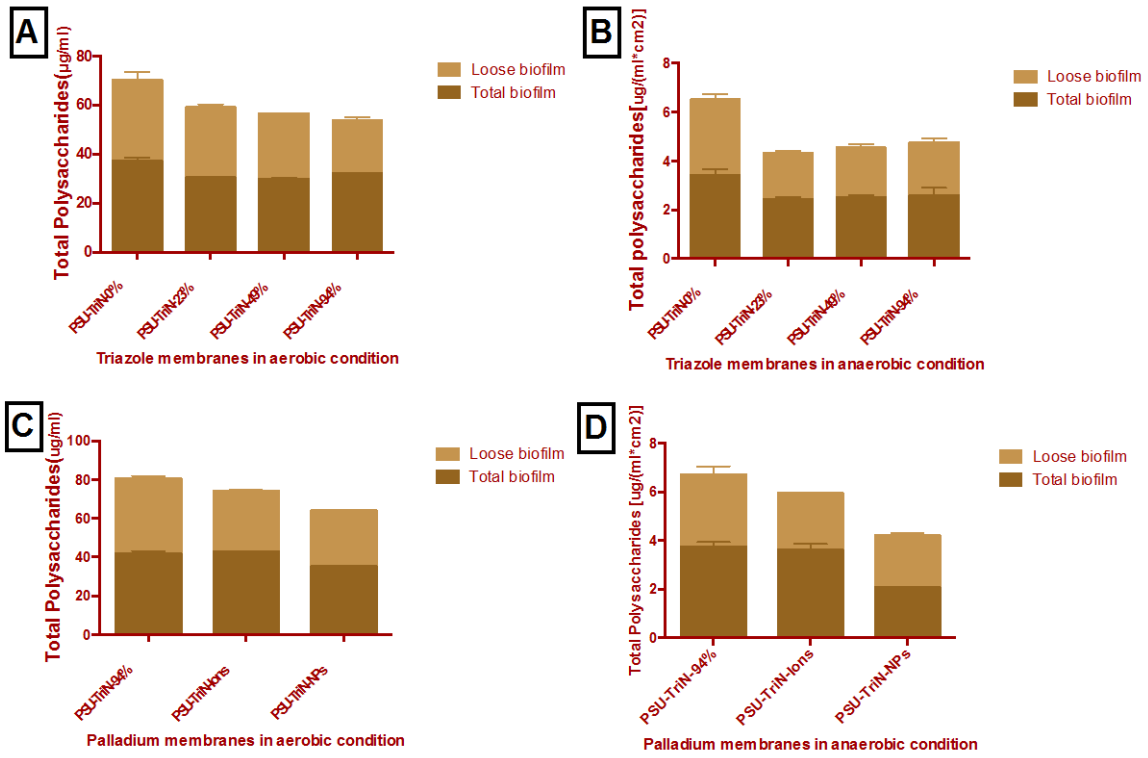

Figure 8. Quantification of total polysaccharides in the biofilm attached on (A)Different concentrations of triazole membranes in aerobic condition. (B)Different concentrations of triazole membranes in anaerobic condition. (C)PSU-TriN-94%, PSU-TriN-Ions, and PSU-TriN-NPs in aerobic condition. (D)PSU-TriN-94%, PSU-TriN-Ions and PSU-TriN-NPs in anaerobic condition.

For proteins, even though there were significant differences between PSU-TriN-0% membranes with PSU-TriN-23%, PSU-TriN-49%, PSU-TriN-94% membranes in anaerobic conditions, there were no significant differences in aerobic condition (Fig. 9A and B). A further comparison of PSU-TriN-94% membranes with PSU-TriN-Ions and PSU-TriN-NPs membranes also showed no significant difference for the expression

of protein in both aerobic and anaerobic conditions. In additions, as it can be seen in Fig. 9C and D, the concentrations of PSU-TriN-Ions membrane were higher than PSU-TriN-94% membrane.

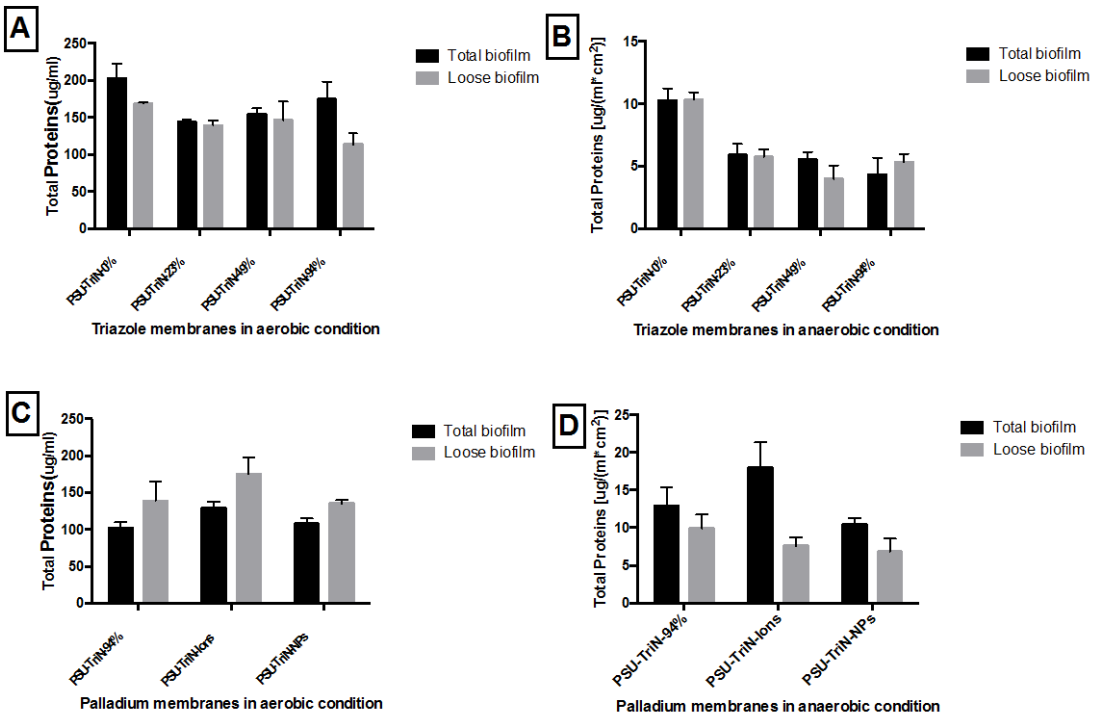

Figure 9. Proteins in biofilm. Similarly, (A)(B) PSU-TriN-0%, PSU-TriN-23%, PSU-TriN-49%, and PSU-TriN-94% were, respectively, in aerobic and anaerobic condition. (C)(D) PSU-TriN-94%, PSU-TriN-Ions and PSU-TriN-NPs were in aerobic and anaerobic conditions.

4.4 Pel polysaccharides quantification

As shown in Fig. 10A, there was lower concentration of Pel polysaccharides on the triazole-modified membranes than PSU membranes. Further analysis by respectively comparing PSU-TriN-0% with PSU-TriN-23%, PSU-TriN-49% and PSU-

TriN-94%, revealed significant differences (t-test, P value were respectively 0.00, 0.00 and 0.03). This implied that triazole membranes could decrease the production of Pel polysaccharides in aerobic condition. A similar observation was made in anaerobic condition (t-test, P=0.00, 0.02, 0.00 respectively). Furthermore, comparing PSU-TriN-94% with PSU-TriN-NPs membranes, we found that triazole membranes embedded with NPs can significantly decrease the production of Pel polysaccharides in both aerobic and anaerobic conditions (Fig. 10C and D) (t-test, P<0.05).

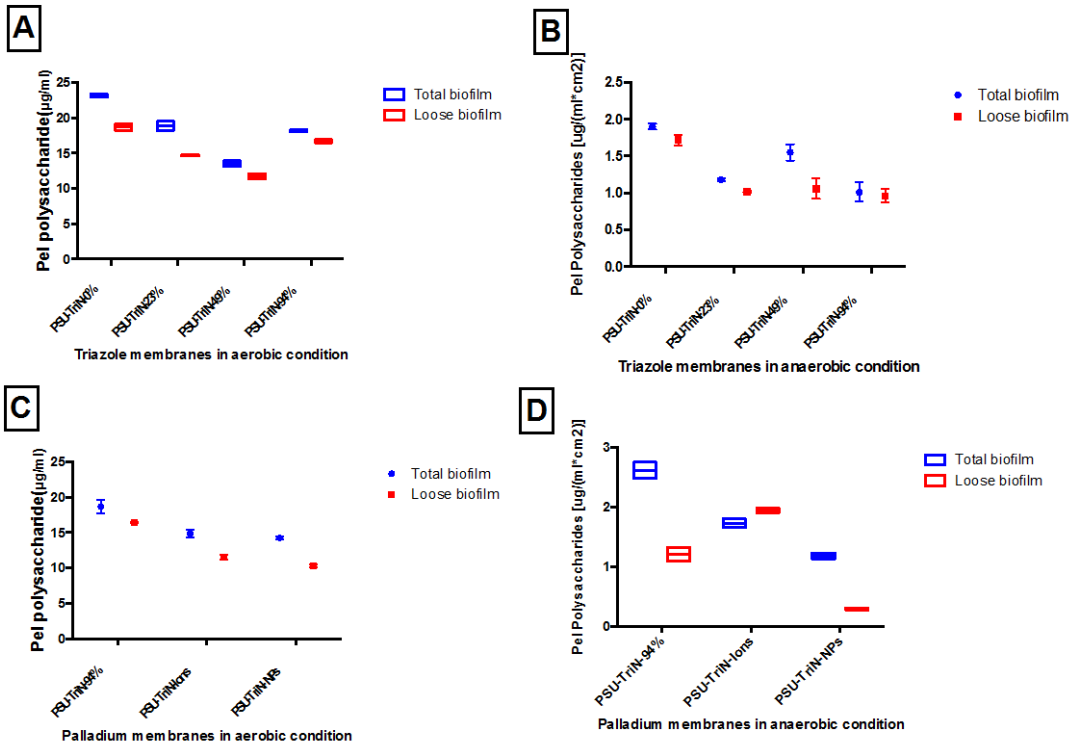

Figure 10. Assessment of Pel polysaccharides product on membranes with (A)different triazole concentrations in aerobic condition; (B)different triazole concentrations in anaerobic condition; (C)PSU-TriN-94%, PSU-TriN-Ions, and PSU-TriN-NPs in aerobic condition; (D)PSU-TriN-94%, PSU-TriN-Ions, and PSU-TriN-NPs in anaerobic condition.

4.5 Demonstration of modified PSU membranes in aerobic membrane bioreactor

Three membranes (i.e. PSU-TriN-0%, PSU-TriN-94% and PSU-TriN-NPs) were connected to an aerobic membrane bioreactor (AeMBR). The membranes were operated for 31 days, with a daily measurement of the transmembrane pressure (TMP) and Chemical Oxygen Demand (COD) removal efficiency calculated every week.

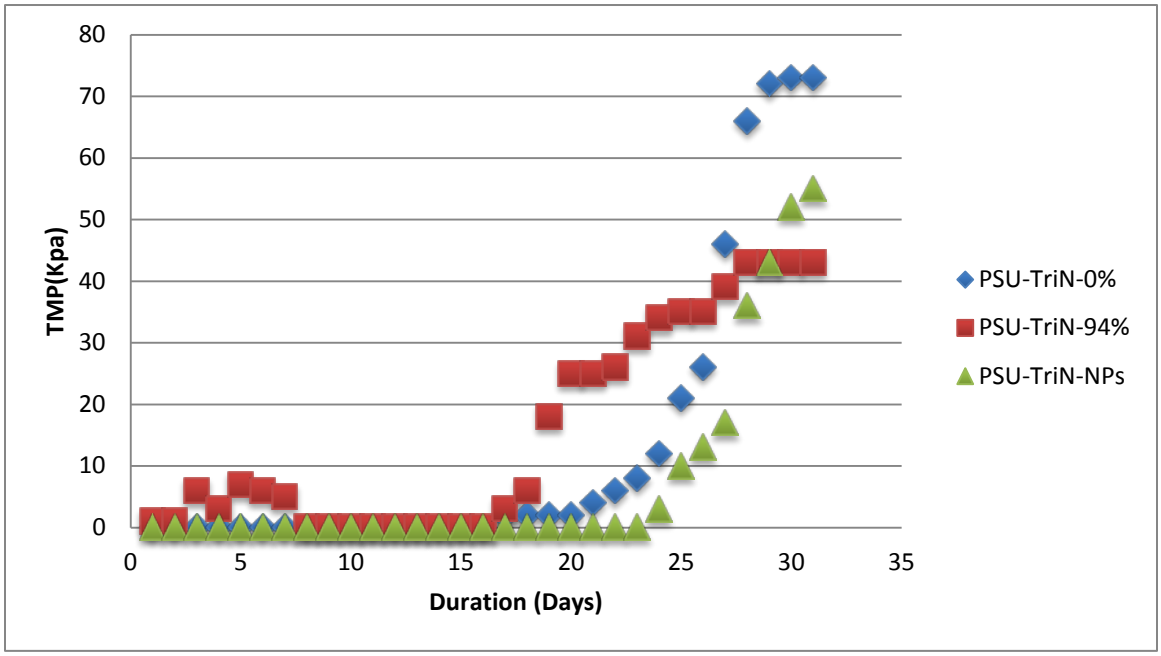

Figure 11. Transmembrane pressure (TMP) measured from membranes integrated to an operating aerobic membrane bioreactor (AeMBR).

All of the three membranes achieved an average COD removal efficiency of 95%. However, as shown in Fig. 11, there was a delay in the TMP increase of PSU-TriN-NPs which suggested a delayed occurrence of biofouling on this membrane compared to the other two membranes. In addition, after the PSU-TriN-0% and PSU-TriN-94% membranes reached critical fouling on the 28th day and 29th day, the TMP dynamics of the PSU-TriN-NPs though increasing, was still in a pre-critical fouling stage (Fig. 11). These TMP plots suggested that the PSU-TriN-NPs membrane had better antifouling effects, and this observation was in concordance with the previous findings illustrated in sections 4.2 through 4.4.

5 Discussions

In this study, results for live/dead ratio of strongly-bound biofilm suggested that triazole-ligand could effectively inhibit growth of bacteria (Fig. 6A and B) in both aerobic and anaerobic conditions. This observation was in agreement with the previous works that demonstrated triazole ligand to have good antibacterial effects---Triazole ligand can interact with cytochrome *P-450* and then inhibit the biosynthesis of ergosterol. Ergosterol is a key compound of bacterial cell membrane. The deficiency of ergosterol will not only affect the activity of membrane bound enzymes but also result in increasing membrane permeability, which ultimately lead to the death of bacterial cells (Van den Bossche et al. 1983; Kathiravan et al. 2012). However, unlike other studies which did not attempt to determine if different concentrations of triazole would result in different antibacterial effect, this study showed no significant differences in the live/dead ratio of microbial cells within the biofilm matrix of PSU membranes (PSU-TriN-0%) with varying triazole concentrations membranes (PSU-TriN-23%, PSU-TriN-49%, PSU-TriN-94%). In addition, we found that majority of the total biofilm was strongly attached on the PSU-TriN-0%, suggesting that PSU-TriN-0% membrane was prone to cell adhesion by bacteria and the subsequent formation of biofilm. The increased susceptibility towards biofouling on the PSU-TriN-0% membranes is likely due to the relatively higher hydrophobicity of this membrane compared to those functionalized with triazoles. It was reported elsewhere that cell surface of bacteria was relatively

hydrophobic. These hydrophobic bacteria would be rejected by hydrophilic membrane but be attracted by hydrophobic membrane (Marshall 1985). Additionally, triazoles were demonstrated to exhibit antibacterial effect (Holla et al. 2005; Aufort et al. 2008; Wang et al. 2010) and hence, the lack of triazole on PSU-TriN-0% to kill the bacteria resulted in a higher live/dead bacterial cell ratio compared to other membranes. Considering all of these together, triazole membranes can successfully inhibit and decrease bacteria attachment on the surface.

In addition, the total polysaccharides and Pel polysaccharides found on PSU-TriN-0% membranes were in higher concentrations than PSU-TriN-23%, PSU-TriN-49% and PSU-TriN-94% membranes. Polysaccharides are the main fraction of EPS, and EPS account for about 90% dry weight of biofilm (Flemming and Wingender 2010). Pel polysaccharides which take up more than fifty percent of polysaccharides are the structural scaffold of P. *aeruginosa* biofilm and act as an important role in cell-to-cell interactions (Ghafoor et al. 2011). Thus, the lower total polysaccharides and Pel polysaccharides concentration between triazole-modified PSU membranes and those without triazole suggest inhibition of biofilm formation in the former set of membranes. Additionally, there were no differences between PSU-TriN-23%, PSU-TriN-49% and PSU-TriN-94% membranes in both total polysaccharides and Pel polysaccharides (Fig. 8 A and B; Fig. 10 A and B). These results were consistent with live/dead ratio and live cells enumeration. They all suggested that PSU-TriN-23%,

PSU-TriN-49% and PSU-TriN-94% exhibited the same antifouling effects despite the differences in triazole concentrations.

This study failed to find any significant differences of protein content in aerobic condition (Fig. 9A), even though a difference in anaerobic condition was found (Fig. 9B). The reasons to account for this observation is unknown. It is likely to be attributed to the broth. In this experiment, we used LB broth, which contains 10 mg/mL tryptone and 5 mg/mL yeast extract. Compared to the protein concentration of EPS, the concentration of protein content in LB broth is high, and may have interfered in the quantification of protein content. Alternatively, the method used to quantify the protein contents is not able to distinguish between proteins that are lysed out of dead bacterial cells and those associated with intact cell membranes. It is possible that the high protein content associated with the triazole-containing PSU membranes were those lysed out from dead bacterial cells due to the antibacterial effect of the triazoles.

Owing to the fact that only PSU-TriN-94% membrane can embed the Pd ions and nanoparticles, we only evaluated PSU-TriN-Ions and PSU-TriN-NPs membranes against PSU-TriN-94% membrane. The addition of Pd ions and nanoparticles onto membranes showed rougher surface topography (Fig. 4 and 5; Tab. 2) due to the presence of the Pd and the difference in the synthesis method compared to the triazole-only membranes. It was previously demonstrated that surface topography can greatly affect biofilm formation (Pang et al. 2005; Park et al. 2005). Membranes with rougher surface are more prone to fouling as roughness can increase the

chance of cell-to-surface interaction and enhance the adhesion of bacteria. Additionally, a rougher surface means a higher shear force, which could lead to tight bacteria attachment (Marshall 1985; Pang et al. 2005). It seemed that the PSU-TriN-Ions and PSU-TriN-NPs membranes were likely to be more prone to fouling than PSU-TriN-0%, PSU-TriN-23%, PSU-TriN-49%, PSU-TriN-94%. However, on the contrary, we found significantly decreased live/dead ratio, live cells, total polysaccharides, and Pel polysaccharides of PSU-TriN-NPs membranes in both aerobic and anaerobic conditions (Fig. 6C and D; Fig. 7C and D; Fig. 8C and D; Fig.10 C and D). These observations suggested that Pd nanoparticles had strong antifouling effects as Pd nanoparticles not only offset the influence of rougher topography but also enhanced the antifouling effects. For PSU-TriN-Ions membrane, more cells may have attached onto this membrane due to the rougher surface, and these cells were then killed by triazole ligands (Holla et al. 2005; Pang et al. 2005). However, no significant differences were observed in its live cells abundance, total polysaccharides, and Pel polysaccharides concentrations when compared to PSU-TriN-94% membranes, indicating that Pd ions do not exhibit any competitive advantage over the mere addition of triazole onto PSU membranes.

6 Conclusions

The results in this study demonstrated that the 1,2,3-triazole modification could inhibit the living cells in biofilm, decrease the expression of Pel polysaccharides and total polysaccharides. The triazole membranes embedded Pd nanoparticles can further extend these effects, even though the embedment makes the surface rougher, which is thought to result in more cell attachment and hence increased biofilm formation. Instead, the Pd nanoparticles embedded membrane shows enhanced antibiofouling effects than triazole modification membrane and PSU membrane.

7 Future works

In this study, we have shown that triazole-modification can enhance the antifouling effects and Pd nanoparticles embedment further improves the anti-biofilm effect from the model bacterium *P. aeroginosa*. However, it is well-documented that many factors can lead to fouling. Such factors include but are limited to the presence of inorganic/organic matter, water flux and TMP, shear rate (Marshall 1985; Gao et al. 2011; Guo et al. 2012). More works need to be performed to verify the potential application of PSU-TriN-NPS membranes in an operating membrane bioreactor system.

We have currently integrated three membranes (i.e. PSU-TriN-0%, PSU-TriN-94% and PSU-TriN-NPs) to an operating AeMBR in our laboratory. The transmembrane pressure profiles shown in Fig. 11 illustrated a delayed membrane biofouling in the presence of Pd nanoparticles on PSU-TriN membranes.

Further work would include the quantification of the EPS and Soluble Microbial Products (SMP), auto-inducers (e.g. AI-2), adenosine triphosphate (ATP) and microbial community on each of the three membranes. It is anticipated that this evaluation of the biofoulant layers on the three membranes integrated to an operating AeMBR will provide more comprehensive insights to how the Pd NPs and triazole can serve to delay membrane fouling events.

REFERENCES

Abràmoff MD, Magalhães PJ, Ram SJ (2004) Image processing with imageJ. Biophotonics Int 11:36–41. doi: 10.1117/1.3589100

Adams CP, Walker K a., Obare SO, Docherty KM (2014) Size-Dependent Antimicrobial Effects of Novel Palladium Nanoparticles. PLoS One 9:e85981. doi: 10.1371/journal.pone.0085981

Aufort M, Herscovici J, Bouhours P, Moreau N, Girard C (2008) Synthesis and antibiotic activity of a small molecules library of 1,2,3-triazole derivatives. Bioorganic Med Chem Lett 18:1195–1198. doi: 10.1016/j.bmcl.2007.11.111

Banerjee I, Pangule RC, Kane RS (2011) Antifouling coatings: Recent developments in the design of surfaces that prevent fouling by proteins, bacteria, and marine organisms. Adv Mater 23:690–718. doi: 10.1002/adma.201001215

Chaplin BP, Reinhard M, Schneider WF, Schüth C, Shapley JR, Strathmann TJ, Werth CJ (2012) Critical review of Pd-based catalytic treatment of priority contaminants in water. Environ Sci Technol 46:3655–3670. doi: 10.1021/es204087q

Cirtiu CM, Dunlop-Brière AF, Moores A (2011) Cellulose nanocrystallites as an efficient support for nanoparticles of palladium: application for catalytic hydrogenation and Heck coupling under mild conditions. Green Chem 13:288. doi: 10.1039/c0gc00326c

Davies DG, Parsek MR, Pearson JP, Iglewski BH, Costerton JW, Greenberg EP (1998) The involvement of cell-to-cell signals in the development of a bacterial biofilm. Science 280:295–298. doi: 10.1126/science.280.5361.295

DuBois M, Gilles K a., Hamilton JK, Rebers P a., Smith F (1956) Colorimetric method for determination of sugars and related substances. Anal Chem 28:350–356. doi: 10.1021/ac60111a017

Dong T, Luo H, Wang Y, Hu B, Chen H (2011) Stabilization of Fe-Pd bimetallic nanoparticles with sodium carboxymethyl cellulose for catalytic reduction of para-nitrochlorobenzene in water. Desalination 271:11–19. doi: 10.1016/j.desal.2010.12.003

Flemming H-C (1997) Reverse osmosis membrane biofouling. Exp Therm Fluid Sci 14:382–391. doi: 10.1016/S0894-1777(96)00140-9

Flemming H-C, Wingender J (2010) The biofilm matrix. Nat Rev Microbiol 8:623–633. doi: 10.1080/0892701031000072190

Forrez I, Carballa M, Fink G, Wick A, Hennebel T, Vanhaecke L, Ternes T, Boon N, Verstraete W (2011) Biogenic metals for the oxidative and reductive removal of pharmaceuticals, biocides and iodinated contrast media in a polishing membrane bioreactor. Water Res 45:1763–1773. doi: 10.1016/j.watres.2010.11.031

Gao W, Liang H, Ma J, Han M, Chen ZL, Han ZS, Li GB (2011) Membrane fouling control in ultrafiltration technology for drinking water production: A review. Desalination 272:1–8. doi: 10.1016/j.desal.2011.01.051

Ghafoor A, Hay ID, Rehm BH a (2011) Role of exopolysaccharides in Pseudomonas aeruginosa biofilm formation and architecture. Appl Environ Microbiol 77:5238–5246. doi: 10.1128/AEM.00637-11

Goeres DM, Hamilton M a, Beck N a, Buckingham-Meyer K, Hilyard JD, Loetterle LR, Lorenz L a, Walker DK, Stewart PS (2009) A method for growing a biofilm under low shear at the air-liquid interface using the drip flow biofilm reactor. Nat Protoc 4:783–788. doi: 10.1038/nprot.2009.59

Guo W, Ngo HH, Li J (2012) A mini-review on membrane fouling. Bioresour Technol 122:27–34. doi: 10.1016/j.biortech.2012.04.089

Hennebel T, Simoen H, De Windt W, Verloo M, Boon N, Verstraete W (2009) Biocatalytic dechlorination of trichloroethylene with bio-palladium in a pilot-scale membrane reactor. Biotechnol Bioeng 102:995–1002. doi: 10.1002/bit.22138

Holla BS, Mahalinga M, Karthikeyan MS, Poojary B, Akberali PM, Kumari NS (2005) Synthesis, characterization and antimicrobial activity of some substituted 1,2,3-triazoles. Eur J Med Chem 40:1173–1178. doi: 10.1016/j.ejmech.2005.02.013

Huang Y, Liu S, Lin Z, Li W, Li X, Cao R (2012) Facile synthesis of palladium nanoparticles encapsulated in amine-functionalized mesoporous metal-organic frameworks and catalytic for dehalogenation of aryl chlorides. J Catal 292:111–117. doi: 10.1016/j.jcat.2012.05.003

Jana NR, Wang ZL, Pal T (2000) Redox catalytic properties of palladium nanoparticles: surfactant and electron donor-acceptor effects. Langmuir 16:2457–2463. doi: 10.1021/la990507r

Juang LC, Tseng DH, Lin HY (2007) Membrane processes for water reuse from the effluent of industrial park wastewater treatment plant: a study on flux and

fouling of membrane. Desalination 202:302–309. doi: 10.1016/j.desal.2005.12.068

Kathiravan MK, Salake AB, Chothe AS, Dudhe PB, Watode RP, Mukta MS, Gadhwe S (2012) The biology and chemistry of antifungal agents: A review. Bioorganic Med Chem 20:5678–5698. doi: 10.1016/j.bmc.2012.04.045

Kim JS, Kuk E, Yu KN, Kim JH, Park SJ, Lee HJ, Kim SH, Park YK, Park YH, Hwang CY, Kim YK, Lee YS, Jeong DH, Cho MH (2007) Antimicrobial effects of silver nanoparticles. Nanomedicine Nanotechnology, Biol Med 3:95–101. doi: 10.1016/j.nano.2006.12.001

Komlenic R (2010) Rethinking the causes of membrane biofouling. Filtr Sep 47:26–28. doi: 10.1016/S0015-1882(10)70211-1

Kustov LM, Finashina ED, Shuvalova E V., Tkachenko OP, Kirichenko O a. (2011) Pd-Fe nanoparticles stabilized by chitosan derivatives for perchloroethene dechlorination. Environ Int 37:1044–1052. doi: 10.1016/j.envint.2011.0

Lien H-L, Zhang W (2005) Hydrodechlorination of Chlorinated Ethanes by Nanoscale Pd/Fe Bimetallic Particles. J Environ Eng 131:4–10. doi: 10.1061/(ASCE)0733-9372(2005)131:1(4)

Lowry G V., Reinhard M (2000) Pd-catalyzed TCE dechlorination in groundwater: Solute effects, biological control, and oxidative catalyst regeneration. Environ Sci Technol 34:3217–3223. doi: 10.1021/es991416j

Marshall KC (1985) Mechanisms of bacterial adhesion at solid± water interface. Bact Adhes ed Savage, DC Fletcher, M pp 133±161 New York: Plenum Press.

Morgan TD, Wilson M (2001) The effects of surface roughness and type of denture acrylic on biofilm formation by Streptococcus oralis in a constant depth film fermentor. J Appl Microbiol 91:47–53. doi: 10.1046/j.1365-2672.2001.01338.x

Nutt MO, Heck KN, Alvarez P, Wong MS (2006) Improved Pd-on-Au bimetallic nanoparticle catalysts for aqueous-phase trichloroethene hydrodechlorination. Appl Catal B Environ 69:115–125. doi: 10.1016/j.apcatb.2006.06.005

Pang CM, Hong P, Guo H, Liu WT (2005) Biofilm formation characteristics of bacterial isolates retrieved from a reverse osmosis membrane. Env Sci Technol 39:7541–7550.

Park N, Kwon B, Kim IS, Cho J (2005) Biofouling potential of various NF membranes with respect to bacteria and their soluble microbial products (SMP):

Characterizations, flux decline, and transport parameters. J Memb Sci 258:43–54. doi: 10.1016/j.memsci.2005.02.025

Rafatullah M, Sulaiman O, Hashim R, Ahmad A (2010) Adsorption of methylene blue on low-cost adsorbents: A review. J Hazard Mater 177:70–80. doi: 10.1016/j.jhazmat.2009.12.047

Rana D, Matsuura T (2010) Surface modifications for antifouling membranes. Chem Rev 110:2448–2471. doi: 10.1021/cr800208y

Randall RJ, Lewis a (1951) The folin by oliver. Readings 193:265–275. doi: 10.1016/0304-3894(92)87011-4

Richardson SD, Plewa MJ, Wagner ED, Schoeny R, DeMarini DM (2007) Occurrence, genotoxicity, and carcinogenicity of regulated and emerging disinfection by-products in drinking water: A review and roadmap for research. Mutat Res - Rev Mutat Res 636:178–242. doi: 10.1016/j.mrrev.2007.09.001

Ruparelia JP, Chatterjee AK, Duttagupta SP, Mukherji S (2008) Strain specificity in antimicrobial activity of silver and copper nanoparticles. Acta Biomater 4:707–716. doi: 10.1016/j.actbio.2007.11.006

Speranza A, Leopold K, Maier M, Taddei AR, Scoccianti V (2010) Pd-nanoparticles cause increased toxicity to kiwifruit pollen compared to soluble Pd(II). Environ Pollut 158:873–882. doi: 10.1016/j.envpol.2009.09.022

Stoodley P, Sauer K, Davies DG, Costerton JW (2002) Biofilms as complex differentiated communities. Annu Rev Microbiol 56:187–209. doi: 10.1146/annurev.micro.56.012302.160705

Toyofuku M, Uchiyama H, Nomura N (2012) Social behaviours under anaerobic conditions in Pseudomonas aeruginosa. Int J Microbiol. doi: 10.1155/2012/405191

Van den Bossche H, Willemsens G, Cools W, Marichal P, Lauwers W (1983) Hypothesis on the molecular basis of the antifungal activity of N-substituted imidazoles and triazoles. Biochem Soc Trans 11:665–667.

Venkatachalam K, Arzuaga X, Chopra N, Gavalas VG, Xu J, Bhattacharyya D, Hennig B, Bachas LG (2008) Reductive dechlorination of 3,3???,4,4???-tetrachlorobiphenyl (PCB77) using palladium or palladium/iron nanoparticles and assessment of the reduction in toxic potency in vascular endothelial cells. J Hazard Mater 159:483–491. doi: 10.1016/j.jhazmat.2008.02.109

Villalobos LF, Karunakaran M, Peinemann K-V (2015) Complexation-Induced Phase Separation: Preparation of Composite Membranes with a Nanometer-Thin Dense Skin Loaded with Metal Ions. Nano Lett 150427133404009. doi: 10.1021/acs.nanolett.5b00275

Villalobos LF, Neelakanda P, Karunakaran M, Cha D, Peinemann K V. (2013) Poly-thiosemicarbazide/gold nanoparticles catalytic membrane: In-situ growth of well-dispersed, uniform and stable gold nanoparticles in a polymeric membrane. Catal Today 236:92–97. doi: 10.1016/j.cattod.2013.10.067

Wang X, Chen C, Liu H, Ma J (2008) Preparation and characterization of PAA/PVDF membrane-immobilized Pd/Fe nanoparticles for dechlorination of trichloroacetic acid. Water Res 42:4656–4664. doi: 10.1016/j.watres.2008.08.005

Wang X-L, Wan K, Zhou C-H (2010) Synthesis of novel sulfanilamide-derived 1,2,3-triazoles and their evaluation for antibacterial and antifungal activities. Eur J Med Chem 45:4631–4639. doi: 10.1016/j.ejmech.2010.07.031

Wong MS, Nutt MO, Kowalski KN, Hughes JB (2005) Designing Pd-on-Au bimetallic nanoparticle catalysts for trichloroethene hydrodechlorination. AIChE Annu Meet Conf Proc 39:9795.

Xie Y, Tayouo R, Nunes SP (2015) Low fouling polysulfone ultrafiltration membrane via click chemistry. J Appl Polym Sci 41549:n/a–n/a. doi: 10.1002/app.41549

Xu KD, Stewart PS, Xia F, Mcfeters G a, Huang C (1998) Spatial Physiological Heterogeneity in Pseudomonas aeruginosa Biofilm Is Determined by Oxygen Availability Spatial Physiological Heterogeneity in Pseudomonas aeruginosa Biofilm Is Determined by Oxygen Availability. 64:4035–4039.

Zhao X, Lv L, Pan B, Zhang W, Zhang S, Zhang Q (2011) Polymer-supported nanocomposites for environmental application: A review. Chem Eng J 170:381–394. doi: 10.1016/j.cej.2011.02.071